Physica B 407 (2012) 1823–1826

Contents lists available at SciVerse ScienceDirect

Physica B

journal homepage: www.elsevier.com/locate/physb

Charge-density fluctuations probed by vibronic modes of $K_{0.3}MoO_3$

Rebecca Beyer*, Neven Barišić, Martin Dressel

Physikalisches Institut, Universität Stuttgart, Pfaffenwaldring 57, 70550 Stuttgart, Germany

ARTICLE INFO

Available online 8 January 2012

Keywords:
Blue bronze
Charge density wave
Fluctuation regimes
Infrared spectroscopy
Stretching vibrations

ABSTRACT

Polarized reflection measurements have been performed on the charge-density-wave compound $K_{0.3}MoO_3$ from room temperature down to $T=50$ K. For the first time, the least conducting direction (perpendicular to the planes of MoO_6-octahedrons) was investigated in the entire infrared range of frequency. The diatomic MoO stretching vibrations centered around 940 cm^{-1} exhibit an unusual temperature dependence; below some characteristic temperature $T^* \approx 200$ K the line shape changes significantly. The observed features are attributed to change-density-wave fluctuations that are present well above the charge-density-wave transition T_{CDW}, and start to develop short-range order at T^*.

1. Introduction

Ever since the discovery of quasi-one-dimensional metals, fluctuation effects became important in theory and experiment. Purely one-dimensional materials cannot exhibit any long-range order such as a charge density wave (CDW) at finite temperatures; only short-range correlations are possible. In contrast, mean-field solutions neglecting any fluctuation effects predict a finite transition temperature T_{MF} below which long range order develops. Real quasi-one-dimensional crystals are strongly anisotropic, three-dimensional materials with interactions in all three directions, and the actual transition temperature for the long-range CDW, T_{CDW}, is significantly lower than T_{MF}, but finite. In quasi-one-dimensional systems that undergo a CDW transition four temperature regimes can be distinguished. At highest temperatures, the charges are distributed uniformly in the crystal. Below the mean-field temperature T_{MF}, fluctuations of the charge density set in but exhibit only short-range order in the metallic direction. Lowering the temperature below the second critical temperature T^* results in a long-range order in the metallic direction and an additional short-range order in the perpendicular directions. Below the transition temperature T_{CDW}, long-range order is established in all three directions [1,2].

Blue bronzes $A_{0.3}MoO_3$ (A=K, Rb, Tl) are model-type quasi-one-dimensional metals which undergo a Peierls-type metal–insulator transition at $T_{CDW} = 183$ K. X-ray scattering investigations clearly prove the formation of a CDW along the b-direction below the transition temperature T_{CDW}. The collective amplitude and phase mode of the CDW were revealed by Raman and optical spectroscopy. Optical methods are a powerful tool to investigate low-dimensional materials as the different crystallographic axes can be easily addressed by polarizing the light in the appropriate direction [3–5].

Here we measure for the first time the blue bronze $K_{0.3}MoO_3$ with light polarized along the least conducting direction, i.e. perpendicular to the building MoO-planes. By carefully analyzing diatomic MoO stretching vibrations, we prove the influence of the charge density fluctuations on the lattice and show that the crossover from one- to two-dimensional fluctuations can be observed by infrared spectroscopy.

2. Stretching vibrations

Usually the formation of a CDW is accompanied by a modulation of the lattice site and the same effect, but much weaker, has to be expected for the onset of charge density fluctuations. One powerful tool to investigate smallest changes of the lattice sites is to analyze vibrational modes for example diatomic stretching vibrations, which are extremely sensitive to the bond length. Several unique properties of these vibrations are important: (i) the resonance frequency of diatomic MoO-stretching vibrations, which have been observed in several materials [7–11], lies in the range of 900 cm^{-1}–1000 cm^{-1} and is therefore higher than any resonance expected from lattice vibrations. Consequently it is easy to identify these vibrations in the spectra. In contrast the resonance frequency of three-atomic Mo–O–Mo vibrations of $\nu_0 \approx 500$ cm^{-1} is much smaller and can hardly be distinguished from phonons or other vibrational modes. (ii) As mentioned before the resonance frequency is very sensitive to the bond length and the coupling strength. Thorough Raman-measurements [12] show an exponential decay of the resonance frequency with increasing bond length, for example lowering the bond length

* Corresponding author. Tel.: +49 71168560254; fax: +49 71168564886.
E-mail addresses: rebecca.beyer@pi1.physik.uni-stuttgart.de (R. Beyer), barisic@pi1.physik.uni-stuttgart.de (N. Barišić), dressel@pi1.physik.uni-stuttgart.de (M. Dressel).

0921-4526/$ - see front matter © 2012 Elsevier B.V. All rights reserved.
doi:10.1016/j.physb.2012.01.040

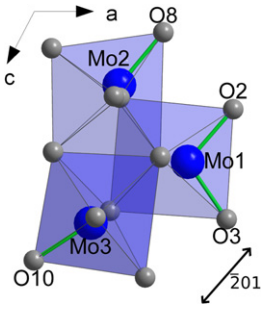

Fig. 1. View on the structure of $K_{0.3}MoO_3$ in the ac-plane. The three different Mo-sites (dark blue circles) are surrounded by eight O-atoms (gray dots) building octahedrons. Four of the 11 different O-sites are bound to only one Mo-site and these MoO-bond (bold green lines) perform high-frequency stretching vibrations. Three of these bonds point almost in the [$\bar{2}$ 0 1]-direction while the last one lies almost perpendicular to the others. (For interpretation of the references to color in this figure legend, the reader is referred to the web version of this article.)

by only 0.01 Å might increase the resonance frequency by up to 20 cm^{-1}.

The exact influence of the CDW on the lattice and therefore on the stretching vibration depends strongly on the character of the CDW. In the incommensurate case the modulation of the lattice sites leads to an infinite number of different bond lengths and therefore the stretching vibration would broaden. In contrast the commensurate case leads to a discrete number of different bond lengths and additional features are expected instead of just a broadening of the corresponding feature.

In the case of the blue bronze there are four bonds capable of performing diatomic stretching vibrations as depicted in Fig. 1. Their resonance frequencies have been measured in Raman and in IR before to $\nu_0(Mo3O10) \approx 975\ cm^{-1}$, $\nu_0(Mo2O8) \approx 910\ cm^{-1}$ and $\nu_0(Mo1O2) \approx \nu_0(Mo1O3) \approx 940\ cm^{-1}$ with $\nu_0(Mo1O2) < \nu_0(Mo1O3)$ [6,16]. Their temperature dependence and the influence of the CDW or charge density fluctuations have not been discussed in detail yet.

3. Experimental methods

Single crystals of $K_{0.3}MoO_3$ with dimensions of $5 \times 3 \times 1\ mm^3$ were measured perpendicular to the natural cleaving plane. To that end, we carefully polished the (1 0 2)-plane spanned by the *b*-direction and the [$\bar{2}$ 0 1]-direction, that is the direction of our main interest. Polarized reflectance measurements in the spectral range from 50 to 12 000 cm^{-1} were performed as a function of temperature using different Fourier-transform infrared spectrometers. In the high-frequency range down to 700 cm^{-1} a Bruker IFS 66v/S spectrometer was utilized equipped with a Hyperion microscope that allowing us to measure a spot size of only 60 μm. To explore the lower frequency range we used the gold-evaporation method; the signal reflected off the full sample area is measured and compared to the signal reflected by a gold film which was evaporated in situ onto the sample. These measurements were performed in a Bruker IFS 113v spectrometer. To compute the optical conductivity we applied a Kramers–Kronig transformation [13] to our data, with the reflectivity extrapolated to zero frequency using the Hagen–Rubens relation for metallic and a constant reflectivity for insulating states. The high frequency range was extrapolated by the relation $R \propto \omega^{-4}$ commonly used.

4. Results and analysis

To characterize the samples, optical measurements along the *b*-direction were performed at different temperatures and compared to previous results [14–18]. In Fig. 2 the reflectivity and optical conductivity for light polarized along the *b*-direction are shown for two temperatures. We did not smooth the noisy room-temperature far-infrared reflectivity data; instead, after performing the Kramers–Kronig transformation, both reflectivity and optical conductivity were fitted simultaneously by Drude and Lorentz terms. As expected for a metal, the low-frequency reflectivity is caused by the Drude response of the free conduction electrons with a scattering rate of $\gamma = 293\ cm^{-1}$. The conductivity $\sigma(\omega \to 0) = 2300\ (\Omega cm)^{-1}$ is consistent with the dc-conductivity reported previously [14]. The mid-infrared region is governed by a broad resonance due to one or more interband transitions. Our results agree with previous reports; the three sharp absorption lines at 400–650 cm^{-1} were assigned to impurity activated modes [17]. The strength of these modes together with the transition temperature give a good measure for the sample quality. From measuring several crystals, we have chosen the specimen for the measurements in [$\bar{2}$ 0 1]-direction that combines the best sample quality and a suitable thickness.

Below the transition temperature $T_{CDW} = 183$ K, the sample turns insulating and the Drude response in the low-frequency part of the spectrum vanishes completely. Instead a large number of phonon modes appear in the spectrum. In $K_{0.3}MoO_3$ the opening of the CDW gap at $2\Delta = 1100\ cm^{-1}$ cannot be observed directly because it develops just in the range of the broad MIR-interband resonance. The optical conductivity at frequencies close to the gap has been discussed by Degiorgi et al. [18].

The reflectivity and the optical conductivity for the [$\bar{2}$ 0 1]-direction is plotted in Fig. 3. The reflectivity remains low over the entire frequency range, except strong phonons in the mid and far-infrared. The conductivity is basically zero up to 3000 cm^{-1}, clearly reflecting the absence of conducting electrons. $K_{0.3}MoO_3$ is an insulator in the [$\bar{2}$ 0 1]-direction and independent on temperature. Consequently there is no sign of the CDW transition observed in the optical properties, in contrast to the dc resistivity which exhibits a clear indication of the CDW gap even in the [$\bar{2}$ 0 1] direction. At high frequencies ($\nu > 3000\ cm^{-1}$) interband transitions expand beyond the measured frequency range and cannot be discussed in detail here.

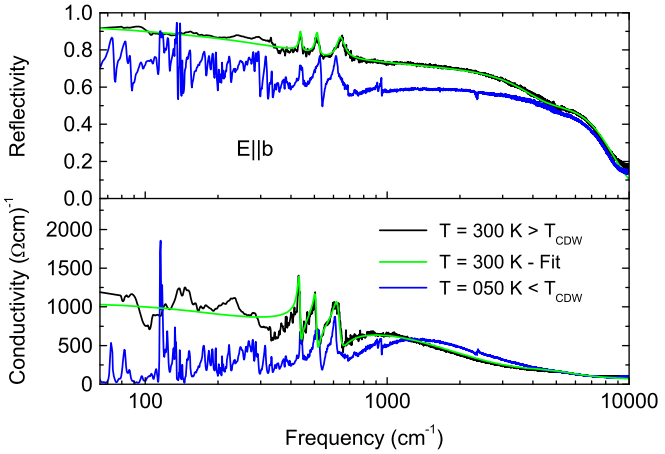

Fig. 2. The reflectivity and the optical conductivity of $K_{0.3}MoO_3$ measured with light polarized along the metallic *b*-direction at room temperature (black) and at T=50 K (blue lines). The reflectivity is high at all temperatures. For $T > T_{CDW} = 183$ K, only three strong features can be identified between 400 and 650 cm^{-1} which are present at all temperatures and attributed to impurity activated modes. The room-temperature spectrum can be described by one Drude- and four Lorentz-terms, as indicated by the light green curve. Below the CDW transition temperature the reflectivity drops and the conductivity approaches zero at low frequencies (blue line). Additionally, a rich phonon spectrum appears in the spectral range below 500 cm^{-1}. (For interpretation of the references to color in this figure legend, the reader is referred to the web version of this article.)

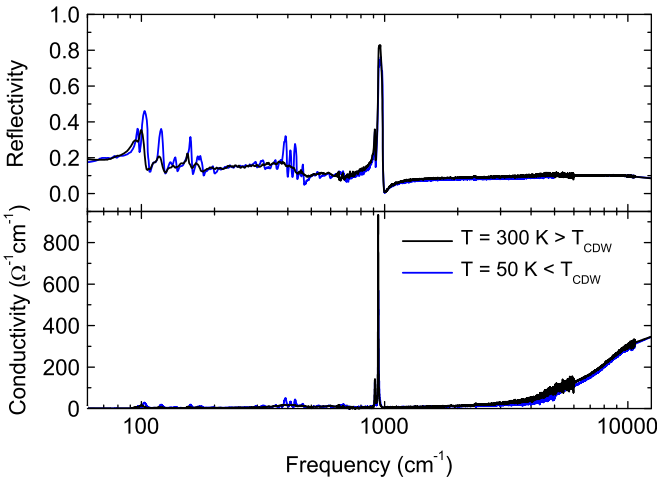

Fig. 3. Optical properties of $K_{0.3}MoO_3$ measured at room temperature (black) and at $T=50$ K (blue) along the least conducting $[\bar{2}\,0\,1]$-direction. The overall reflectivity and conductivity do not change much upon lowering the temperature, typical for insulating materials. The changes in the phonon spectrum are shown in detail in Fig. 4. (For interpretation of the references to color in this figure legend, the reader is referred to the web version of this article.)

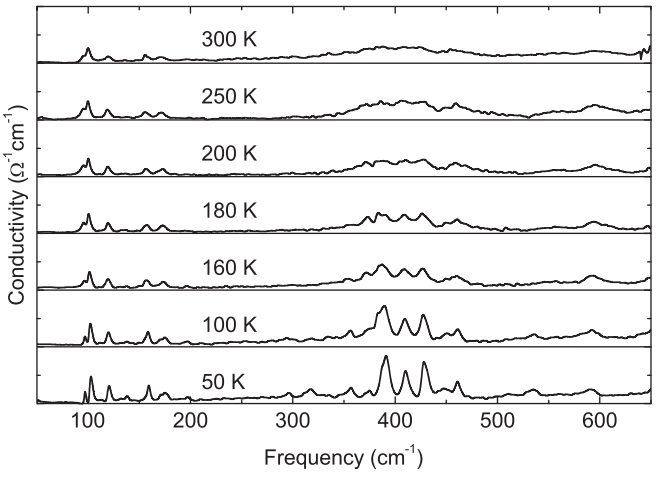

Fig. 4. Detailed view on the phonon spectrum of $K_{0.3}MoO_3$ in $[\bar{2}\,0\,1]$-direction for all temperatures measured. All phonons show a temperature dependence as expected upon cooling down: the resonance frequencies shift to lower frequencies and the linewidth gets smaller. There are no sudden changes below 10 K that would indicate an influence of the CDW on the lattice phonons.

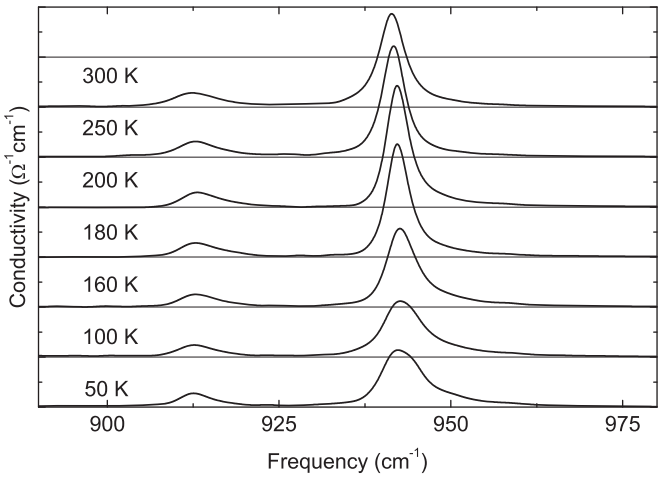

Fig. 5. Detailed view on the MoO stretching vibrations between 890 cm^{-1} and 980 cm^{-1}. The different temperatures have been shifted for clarity. While the feature at 912 cm^{-1} shows only a weak temperature dependence becomes the second feature at 940 cm^{-1} clearly asymmetric at low temperatures. The first feature has been assigned to the Mo2O8 vibration while the second one consists of several vibrations of the O2Mo1O3-system influenced by the formation of the CDW.

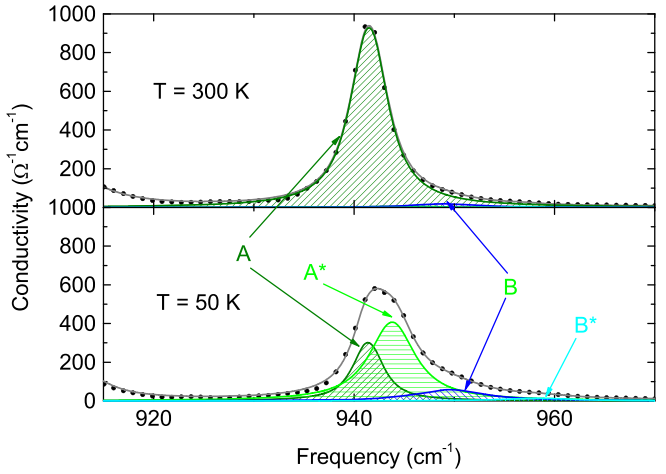

Fig. 6. The mode at 940 cm^{-1} was fitted by several Lorentz-terms. At $T=300$ K (upper frame) one Lorentz term (A) dominates the response. It can be assigned to the Mo1O2 stretching vibration. At this temperature the Mo1O3-bond does not contribute to the signal (feature B). At $T=50$ K (lower frame) the CDW is fully developed and several effects can be observed: feature B has grown much stronger as the bond rotated out of the $[\bar{2}\,0\,1]$-direction. Two additional features (A*, B*) arised as the sites get modulated by the commensurate CDW.

We are able to describe all phonon features completely by a sum of Lorentz terms. This procedure is done at all temperatures. However, a full assignment of all the vibrational features below 1000 cm^{-1} is beyond the scope of this paper. Already from Fig. 4 it can be seen, that none of the features observed below 500 cm^{-1} shows any unusual temperature dependence; no abrupt changes are found at or below the CDW transition temperature.

In contrast, the high-frequency feature at 940 cm^{-1} related to the MoO stretching vibration becomes asymmetric below T_{CDW} as shown in Fig. 5. We could fit the 912 cm^{-1} mode by a single Lorentz term. The 940 cm^{-1} feature, however consists of one strong (A in Fig. 6) and one very weak (B) Lorentz term. At low temperatures, two additional Lorentz terms (A* and B*) are required in order to achieve a good agreement between data and fit.

5. Discussion

Previous considerations in Section 2 allow us to assign the measured features. Obviously the vibration at 912 cm^{-1} is the response of the Mo2O8 stretching vibration while peak A (see Fig. 6) has its origin in the Mo1O2-vibration and the much weaker Peak B resembles the Mo1O3 stretching vibration.

In order to understand the effects the developing CDW has on the lattice and therefore on the MoO-bonds, we calculate the spectral weight of each of the four features A, A*, B, B* for all temperatures and present the results in Fig. 7.

The first observation is, that the spectral weight of feature A rises a lot under cooling. We explain this effect with changes of the Mo1O3-bond leading to a stronger dipole moment pointing in the direction measured.

The second effect is the rise of two additional features A* and B*. Their resonance frequencies are higher than those of the

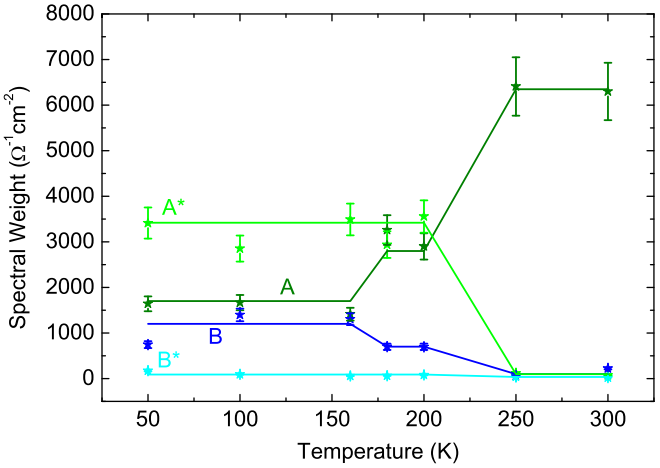

Fig. 7. The spectral weight of the features A, B, A* and B*. One can clearly see that the changes set in at temperatures much higher than the transition temperature.

original features A and B. As discussed before an incommensurate CDW would lead to a continuous modulation of the lattice sides and a broadening of the features A and B would be expected. In contrast we observe two new and discrete features resembling a commensurate CDW. The wavevector of the CDW in $K_{0.3}MoO_3$ is $q=0.7485$b, so it is incommensurate but very close to the commensurate value of $q=0.75$b. From our measurements in b-direction we know that a certain amount of impurities are present in our crystals; hence the CDW is likely to be pinned to these imperfections leading to a commensurate CDW and discrete bond lengths. Interestingly, this also holds for CDW fluctuations. We should recall here that paraconductivity including indications of a collective pinned-mode resonance was observed along the chain direction b well above T_{CDW}, too [14,15].

The most remarkable observation is that both effects mentioned above already set in at temperatures much higher than T_{CDW}. Thus we conclude that both effects can be triggered not only by a fully established CDW but also by charge-density fluctuations. The orientation of the investigated bonds perpendicular to the planes of the MoO_6-octahedrons makes them especially sensitive to changes in this directions such as the onset of short-order fluctuations perpendicular to the planes at T^*. From our investigations we estimate $T^* \approx 200$ K as the temperature where charge fluctuations set in and lead to a distortion of the 940 cm^{-1} mode. These conclusions are in agreement with previous structural investigations [19].

6. Conclusion

We have performed infrared measurements on the least-conducting [$\bar{2}$ 0 1]-direction of the blue bronze $K_{0.3}MoO_3$ as a function of temperature. The stretching vibrations of diatomic MoO-bonds are very sensitive to structural changes, and hence they provide a powerful tool to investigate the fluctuation regimes of materials consisting of planes of MoO_6-octahedrons. By carefully analyzing the temperature evolution of these vibrations, we were able to estimate the onset of two-dimensional correlations to $T^* \approx 200$ K.

References

[1] L.P. Gor'kov, G. Grüner (Eds.), Charge Density Waves in Solids, North-Holland, Amsterdam, 1989.
[2] G. Grüner, Density Waves in Solids, Addison-Wesley, Reading, MA, 1994.
[3] P. Monceau (Ed.), Electronic Properties of Inorganic Quasi-One-dimensional Compounds, vols. I and II, Reidel, Dordrecht, 1985.
[4] G. Grüner, Rev. Mod. Phys. 60 (1988) 1129.
[5] C. Schlenker (Ed.), Low-dimensional Electronic Properties of Molybdenum Bronzes and Oxides, Kluwer Academic Publishers, Dordrecht, 1989.
[6] S. Nishio, M. Kakihana, Phys. Rev. B 63 (2001) 033104.
[7] G. Travaglini, P. Wachter, J. Marcus, C. Schlenker, Solid State Commun. 42 (1982) 407.
[8] S. Jandl, M. Banville, C. Pepin, J. Marcus, C. Schlenker, Phys. Rev. B 40 (1989) 12487.
[9] K. Eda, J. Solid State Chem. 83 (1989) 292.
[10] D. Yin, C. Li, J. Wang, R. Xiong, J. Shi, C. Bi, J. Ma, X. Qiu, J. Phys. Chem. Solids 70 (2009) 249.
[11] L. Seguin, M. Figlarz, R. Cavagnat, J.-C. Lassègues, Spectrochim. Acta A 51 (1995) 1323.
[12] F.D. Hardcastle, I.E. Wachs, J. Raman Spectrosc. 21 (1990) 683.
[13] M. Dressel, G. Grüner, Electrodynamics of Solids, Cambridge University Press, Cambridge, 2002.
[14] B.P. Gorshunov, A.A. Volkov, G.V. Kozlov, L. Degiorgi, A. Blank, T. Csiba, M. Dressel, Y. Kim, A. Schwartz, G. Grüner, Phys. Rev. Lett. 73 (1994) 308.
[15] A. Schwartz, M. Dressel, B. Alavi, A. Blank, S. Dubois, G. Grüner, B.P. Gorshunov, A.A. Volkov, G.V. Kozlov, S. Thieme, L. Degiorgi, F. Lévy, Phys. Rev. B 52 (1995) 5643.
[16] G. Travaglini, P. Wachter, in: Gy. Hutiray, J. Solyom (Eds.), Charge Density Waves in Solids, Lecture Notes in Physics, vol. 217, 1985, p. 115.
[17] G. Travaglini, P. Wachter, J. Marcus, C. Schlenker, Solid State Commun. 37 (1980) 599.
[18] L. Degiorgi, B. Alavi, G. Mihály, G. Grüner, Phys. Rev. B 44 (1991) 7808.
[19] J.P. Pouget, C. Escribe-Filippini, B. Hennion, R. Currat, A.H. Moudden, R. Moret, J. Marcus, C. Schlenker, Mol. Cryst. Liq. Cryst. 121 (1985) 111.